Kinetics and Equilibrium of Multicomponent Adsorption on Chiraly Templated Surfaces

PAWEŁ SZABELSKI,[1] JULIAN TALBOT[2]
[1]*Department of Theoretical Chemistry, Faculty of Chemistry, Maria Curie-Skłodowska University, Pl. M.C. Skłodowskiej 3, 20-031 Lublin, Poland*
[2]*Department of Chemistry and Biochemistry, Duquesene University, Pittsburgh, Pennsylvania 15282-1530*

Received 10 May 2004; Accepted 25 June 2004
DOI 10.1002/jcc.20107
Published online in Wiley InterScience (www.interscience.wiley.com).

Abstract: In this contribution we propose a simple model of adsorption of a binary (racemic) mixture on a chiraly templated surface. As an example, the adsorption of a liquid mixture of enantiomers on a chiral stationary phase (CSP) is considered. In particular, we study the effect of the lateral interactions in the adsorbed phase on the kinetic and equilibrium isotherms of the enantiomers. Additionally, we investigate the influence of the composition of the surface on the performance of the CSP in the presence of the lateral interactions. To that end, the adsorption of the mixture is modeled by using Monte Carlo simulations as well as by applying an analytical approach involving rate equations coupled with the Mean Field Approximation (MFA). The predictions of the theory are found to be in good agreement with the results of the simulations.

 J Comput Chem 25: 1779–1786, 2004

Key words: chiral surfaces; adsorption; Monte Carlo simulations; racemic mixtures; lateral interactions

Introduction

Adsorption on chiraly templated surfaces has recently become one of the most intensively studied topics in interface science. This refers particularly to heterogeneous catalysis where chiral surfaces are produced either by precise cutting of metallic crystals[1,2] or by irreversible adsorption of chiral molecules on catalitically active metals like platinum,[3] palladium,[4] copper,[5,6] or nickel.[7,8] Chiraly templated surfaces prepared in such ways can serve as, for example, highly enantioselective catalysts enabling production of a desired enantiomeric form of a chiral molecule.[9] On the other hand, chiraly templated surfaces can be also fabricated by bonding chiral molecules to nonmetallic surfaces like, for example, silica. Materials of this type are called chiral stationary phases (CSPs), and they are commonly used in chiral chromatography to purify or separate components of racemic mixtures. In this case, separations of enentiomeric pairs by adsorption processes seem more beneficial compared to other methods like fractional crystallization or asymmetric synthesis, which are either tedious and expensive or they give products of lower purity.

Adsorptive separation of enantiomers has been long recognized as a powerful method that is frequently used in different branches of chemistry and biochemistry. One of the most versatile techniques is high-performance liquid chromatography (HPLC) in both analytical and preparative modes.[10–12] It is worth noting that, among many types of chromatographic separations, the separation of enantiomers by HPLC is of special importance because it is usually required to provide very high-purity products. This comes from the fact that most of the enantiomers separated and purified by HPLC are used in drug, cosmetic, and pharmaceutical industries. The major risk in this case is the fact that one enantiomeric form of the same substance may exhibit desired metabolic behavior while the other may be a serious health hazard. For this reason, a detailed understanding of the mechanism of adsorption of enantiomers in HPLC seems indispensable for predicting and eliminating possible effects leading to deterioration of the separation.

The CSPs used in chromatography to separate enantiomers usually consist of an achiral matrix (e.g., porous silica) with bonded chiral ligands. Among them, the most prevalent are small groups (e.g., Pirkle phases) or macromolecules, including cellulose derivatives[13–17] and proteins.[18,19] Despite different physicochemical properties of various CSPs, enantioselective adsorption processes carried out in their presence are controlled by the same or very similar mechanisms. Specifically, the adsorption on CSPs is usually considered to take place on two kinds of sites that are

Correspondence to: P. Szabelski; e-mail: szabla@vega.umcs.lublin.pl
Contract/grant sponsor: Rector of Maria Curie-Skłodowska University.

common for all types of the stationary phases mentioned above: chiral receptors (chiral ligands), which are responsible for the selective differentiation between the components of the racemic mixture and the "background" nonselective sites (achiral matrix).

The above picture of the CSP has been used to build the so-called biLangmuir (bL) model of adsorption, which can describe correctly adsorption of racemic mixtures in different experimental systems.[10,13–17,19] In the bL model, both enantiomers adsorb from solution in a localized way (no surface diffusion is allowed) such that they form a mixed monolayer on the surface. Furthermore, it is assumed that one adsorption site can be occupied by at most one molecule of the adsorbate. Because the adsorption on each kind of site is competitive and lateral interactions in the absorbed phase are assumed to be absent, the adsorption isotherm of a given enantiomer is a simple linear combination of two competitive Langmuir isotherms associated with adsorption on the selective and nonselective sites, that is

$$q_i = \frac{q^*_{si} c_i k^s_i}{1 + c_1 k^s_1 + c_2 k^s_2} + \frac{q^*_{ni} c_i k^n_i}{1 + c_1 k^n_1 + c_2 k^n_2} \quad \text{for} \quad i = 1, 2 \quad (1)$$

where q_i is the amount adsorbed of enantiomer i, c_1 and c_2 are the concentrations of the enantiomers in solution, q^*_{si} and q^*_{ni} are the saturation capacities of the selective and nonselective sites for a given enantiomer and k^s_i and k^n_i are the associated equilibrium adsorption constants. To maintain thermodynamic consistency it is usually assumed that $q^*_{s1} = q^*_{s2}$ and $q^*_{n1} = q^*_{n2}$, which means that the adsorption sites are equally accessible for both enantiomers.

Although widely used to model chiral separations in chromatography, the bL model is only an idealized representation of the adsorption processes taking place in real systems. In particular, it disregards factors such as energetic heterogeneity of the adsorbing surface and interactions between adsorbed molecules. For example, in the case of adsorption of *rac*-1-phenyl-1-propanol on cellulose tribenzoate it has been shown that the extended version of the bL model, which accounts for the surface heterogeneity, gives more accurate predictions of the adsorption isotherms compared to the original bL model.[14] Similarly, it has been deduced from experimental data that lateral interactions may be responsible for some peculiarities observed in the adsorption isotherms. For example, strong attractive interactions may, in general, produce downward convexity of adsorption isotherms—unusual behavior that has been observed for different solutes including toluene and butyl benzene[20] or butyl benzoate.[21] Obviously, this phenomenon may also have considerable influence on the separation of enantiomers. For this reason, it seems worthwhile to examine how lateral interactions affect adsorption of enantiomeric mixtures on CSPs.

With this purpose in mind, in this article we study the adsorption of a racemic mixture on a model chiral adsorbent, taking into account the lateral interactions in the adsorbed phase. Special attention is paid to the influence of the interactions on the effectiveness of the enantiomer separation. Additionally, we study the effect of the composition of the surface, that is, the fraction of the selective sites, on the adsorption isotherms of enantiomers. The results presented here refer to both kinetic and equilibrium aspects of the adsorption process.

Theory

The surface of the stationary phase considered here consists of two types of adsorption sites: nonselective centres (n) and chiral selectors (s). Sites of both kinds are randomly distributed on a square lattice, and their relative concentrations are f^n and f^s, respectively. Sites of the first type correspond to the achiral matrix, which is unable to resolve the enantiomers. The sites of the latter type, however, are assumed to be able to differentiate between the enantiomers, which we label 1 and 2. Despite the different adsorption properties of the sites, each of them is allowed to accommodate at most one molecule of the adsorbate. In the following, we assume that the second component (2) of the mixture is always more strongly adsorbed by the selective sites, while both enantiomers interact with equal strength with the nonselective sites. We also assume that the adsorption energy for the nonselective sites is always lower than for the selective sites, regardless of the type of enantiomer adsorbed. Accordingly, the following relation between the associated equilibrium adsorption constants holds: $k^n < k^s_1 < k^s_2$.

The lateral interactions in the adsorbed phase are assumed to be short-ranged and, furthermore, entirely symmetrical. This means that the strength of interactions is not dependent on the type of interacting enantiomers (1-1, 1-2, or 2-2) or on the type of adsorption site (s or n) but is determined by just one energy parameter, ε, that is the same for all adsorbed pairs of enantiomers. These simplifications are, to some extent, supported by the results of computer simulations of thermodynamic and structural properties of racemic mixtures.[22,23] In particular, it has been found that the excess properties, including excess volume and enthalpy, of the primitive model of a racemic mixture are negligible.[25] Consequently, as a first approximation, molecular interactions in a racemic mixture can be treated as being very similar to those existing in a bulk phase of either of the pure enantiomers. We believe that this property also applies the adsorbed phase.

Taking into account the above assumptions and using the Mean Field Approximation (MFA),[24] the adsorption kinetics may be described by the following system of four ordinary differential equations:

$$\frac{d\theta^x_i}{dt} = k^x_{ai} c_i (f^x - \theta^x_1 - \theta^x_2) - k^x_{di} \theta^x_i \Phi \quad i = 1, 2 \quad x = s, n \quad (2)$$

where θ^x_i is the coverage of sites x by ith component, c_i is the concentration of ith component in the solution, k^x_{ai} and k^x_{di} are the associated adsorption and desorption rate constants, respectively, and t denotes time. The above equations are coupled by the interaction term

$$\Phi = \exp\left(z\varepsilon \sum_{i,x} \theta^x_i\right) = \omega^{z\theta_t} \quad (3)$$

where θ_t is the total surface coverage, z is the coordination number of the lattice, equal to 4 in our case, and $\omega = \exp(\varepsilon/kT)$ is the interaction parameter that is less than 1 for attractive interactions ($\varepsilon < 0$) and greater than 1 for repulsive interactions ($\varepsilon > 0$).

The system of kinetic equations given by eq. (2) can be solved numerically for a particular set of parameters with no difficulty. However, to compare the kinetic isotherms obtained from the theory with the results of the MC simulation one has to define a suitable time unit, t^*, which is common for both methods. Obviously, such a definition is somewhat arbitrary and can be provided in many ways, especially for adsorption of multicomponent mixtures on homogeneous surfaces.[25] For example, when the surface is homogeneous one can set $t^* = c_i k_{ai} t$, where the index i refers to an arbitrarily chosen component of the mixture (reference component). However, when the surface is heterogeneous not all of the choices of the reduced simulation time are equally convenient with respect to the MC simulations. To solve this problem, without loss of generality, in this study we set

$$k^s_{a1} = k^n_{a1} = k_{a1} \quad \text{and} \quad k^s_{a2} = k^n_{a2} = k_{a2} \tag{4}$$

such that

$$t^* = t(k_{a1}c_1 + k_{a2}c_2) \tag{5}$$

which simplifies the MC algorithm and makes the simulation results directly comparable with the theory. Using the time unit defined in eq. (5) one may rewrite eq. (2) in the following form

$$\frac{d\theta^x_i}{dt^*} = \alpha_i(f^x - \theta^x_1 - \theta^x_2) - k^*_{di}\theta^x_i\Phi \tag{6}$$

where

$$\alpha_i = \frac{k_{ai}c_i}{k_{a1}c_1 + k_{a2}c_2} \quad \text{and} \quad k^{x*}_{di} = \frac{k^x_{di}}{k_{a1}c_1 + k_{a2}c_2} \tag{7}$$

The rate equations presented above were solved numerically using a fourth-order Runge–Kutta method with a time step of 0.01. In particular, numerical solution of eq. (6) generated kinetic isotherms, $\theta_i(t^*) = \theta^s_i(t^*) + \theta^n_i(t^*)$ at a fixed composition of the mixture in solution. Additionally, the equilibrium adsorption isotherms, $\theta_i(t^* \to \infty) = \theta_i$ were found from the stationary solution of eq. (6), which reads

$$\theta_i = \frac{1}{2}f^n \frac{ck^n\Phi}{1 + ck^n\Phi} + f^s \frac{ck^s_i\Phi}{2 + c(k^s_1 + k^s_2)\Phi} \quad i = 1, 2 \tag{8}$$

where

$$k^n = \frac{k^n_{ai}}{k^n_{di}} \quad \text{and} \quad k^s_i = \frac{k^s_{ai}}{k^s_{di}} \tag{9}$$

Moreover, because we are dealing with a racemic (i.e., equimolar) mixture, we set $c_1 = c_2 = 0.5c$, where c denotes the concentration of the racemate in solution. Obviously, the theory may be easily adapted to a binary mixture of any composition.

Simulation

The adsorption kinetics of the mixture was modeled using an $L \times L$ lattice of discrete sites with periodic boundary conditions. Before the actual simulation started, the adsorption and desorption constants of each site were generated according to a preselected rule. As mentioned in the previous section, in this study we assumed that the chiral surface consists of two types of adsorption sites that are spatially distributed on the surface in a random way. To satisfy this requirement, the selective sites at fraction f^s were randomly picked out in the lattice. According to eq. (2), each of these sites was characterized by two adsorption constants, k_{a1} and k_{a2}, and two desorption constants, k^s_{d1} and k^s_{d2}. Similarly, the rest of the lattice sites, that is, the nonselective sites, were characterized by k_{a1} and k_{a2} for adsorption and by k^n_{d1} and k^n_{d2} for desorption. Because the lateral interactions in the adsorbed phase were assumed to be short ranged, only the nearest neighbors of an adsorbed molecule were checked during the simulation.

Let us now present a brief description of the simulation technique; a more detailed presentation can be found elsewhere.[25–28] In the first step of the simulation a lattice site is selected at random. Whenever the site is vacant, a molecule of type i ($i = 1, 2$) is added to the site with a probability α_i. Otherwise, the trial ends. In the next step, each molecule adsorbed on the surface is removed with a probability $\omega^m k^{x*}_{di}/L^2$ ($x = s, n$) where $m \leq z$ is the number of occupied nearest neighbor sites of the molecule. The above procedure, which corresponds to a single simulation step, is repeated several times until the desired coverage is reached. The elapsed time after N simulation steps is $t^* = N(k_{a1}c_1 + k_{a2}c_2)/L^2$. All the simulations described in this work were performed on a lattice with L varying from 30 to 50. The MC results presented in the next section are averages over up to 50 independent runs.

Results and Discussion

In CSPs used in HPLC up to 20% of the receptors may, in special cases, be chiral.[19] Accordingly, we performed simulations for f^s equal to 0.05 and 0.2. The other parameters were taken as: $k_{a1} = 0.2$, $k_{a2} = 0.4$, $k^s_{d1} = 0.05$, $k^s_{d2} = 0.025$, $k^n_{d1} = 0.1$, $k^n_{d2} = 0.2$. The resulting equilibrium adsorption constants [see eq. (9)] were $k^n = 2$, $k^s_1 = 4$ and $k^s_2 = 16$ such that the assumed condition $k^n < k^s_1 < k^s_2$ was satisfied. Because we focus primarily on the effect of ω and f^s on the adsorption process, a detailed discussion of the influence of the rate constants is omitted in this article. However, it can be found elsewhere.[25] We remind the reader that the results are illustrative only and they do not correspond to any particular experimental system. Nevertheless, they reflect qualitative changes in the system behavior that are induced by changes in both strength of the lateral interactions and the receptor concentration.

Figure 1 shows the kinetic adsorption isotherms obtained by the MC simulations (symbols) and the isotherms predicted by the theory (lines). The top part presents the results obtained for $f^s = 0.05$, while the bottom part corresponds to $f^s = 0.2$. In both cases the total concentration of the racemate, c, was equal to 1. The isotherms shown in both parts of Figure 1 were calculated for $\omega = 0.4$, 0.8, and 1.8. As can be seen in the figure, the shape of the

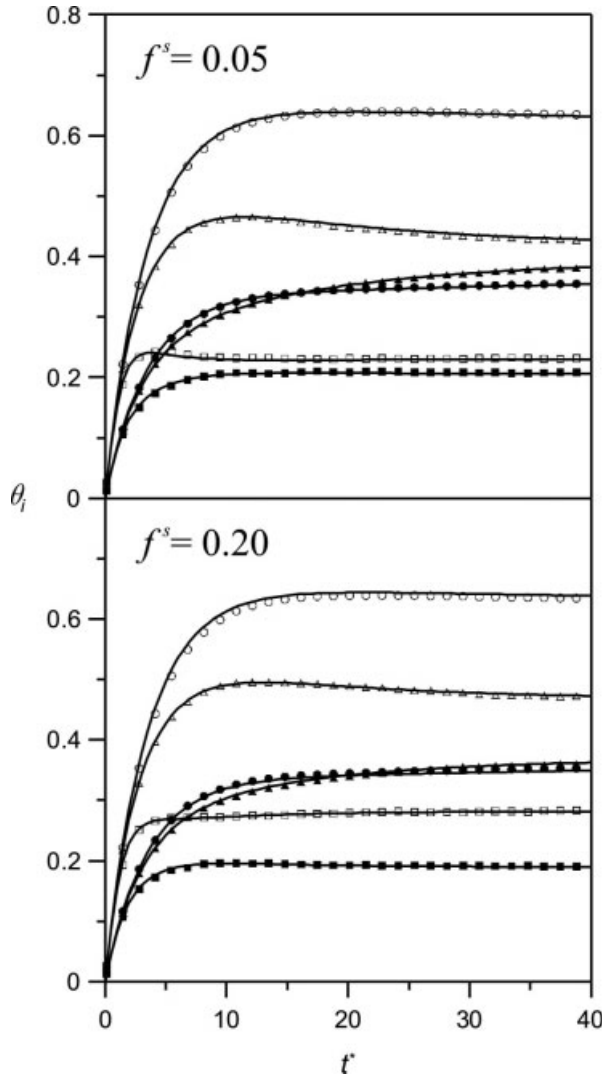

Figure 1. Kinetic adsorption isotherms of components 1 and 2 obtained for different values of the interaction parameter, ω, for the total concentration of the mixture equal to 1. The symbols denote simulation data, while the lines are the results obtained by numerical integration of the rate equations. The isotherms shown in both parts were simulated for ω equal to 0.4 (circles), 0.8 (triangles), and 1.8 (squares). The filled and open symbols refer to components 1 and 2, respectively.

adsorption isotherms is, in general, strongly affected by the strength of lateral interactions. In particular, for both $f^s = 0.05$ and $f^s = 0.2$ we observe that $\theta_2(t^*)$ decreases gradually when ω increases (open symbols). On the other hand, $\theta_1(t^*)$ displays the same tendency only for $t^* < 15$ (top part) and $t^* < 20$ (bottom part). At these points the relative position of the isotherms corresponding to $\omega = 0.4$ (filled circles) and 0.8 (filled triangles) is inverted. It is also worth noting, that for $\omega = 0.8$ and 1.8 the isotherms corresponding to the second component exhibit nonmonotonic behavior. In this case, each of the functions passes through a maximum and reaches its corresponding plateau after sufficiently long time. As seen in Figure 1, the maximum is slightly more evident for stronger repulsive interactions (larger ω) and for smaller f^s (compare the top and the bottom part). Note also, that for $f^s = 0.2$ the distance between θ_2 and θ_1 taken at t^* equal to, say 20 or 30 is larger than for $f^s = 0.05$. The only exception is the case $\omega = 0.4$, for which the distance remains approximately the same when the receptor concentration increases. The above observations indicate two things. First, an increase in f^s improves the separation of enantiomers in the initial stage of adsorption unless attractive interactions in the adsorbed phase are not too strong. Second, for relatively short times, the repulsive interactions in our system are responsible for the deterioration of the separation as well as the decrease in the total amount adsorbed. We also note that the predictions of the proposed theory are in good agreement with the simulation data discussed so far.

To better illustrate the influence of f^s and ω on the efficiency of the separation of enantiomers in Figure 2 we plotted the kinetic selectivity defined as

$$S(t^*) = \frac{\theta_2(t^*)}{\theta_1(t^*)} \tag{10}$$

Let us first consider the top part of Figure 2, where we display the kinetic selectivity as a function of the reduced time, for $f^s = 0.05$. To maintain consistency with Figure 1 the simulation data corresponding to a given ω are plotted using filled symbols from Figure 1. In Figure 2 we display also the selectivities obtained for $\omega = 0.6$ and for $\omega = 1$ (i.e., for the system with no lateral interactions). These additional data are represented by pluses and crosses, respectively. As can be seen from the figure, strong attractive inter-

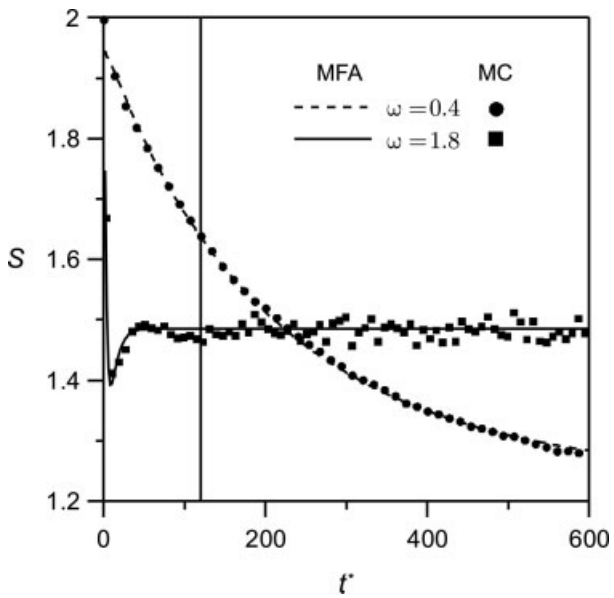

Figure 2. Kinetic selectivity, θ_2/θ_1, as a function of the reduced time, obtained for different values of the interaction parameter, ω, for the total concentration of the mixture equal to 1. The symbols denote simulation data, while the lines are predictions of the theory. The results shown in both parts were simulated for ω equal to 0.4 (●), 0.6 (+), 0.8 (▲), 1.0 (×) and 1.8 (■).

actions are responsible for the fact that the kinetic selectivity is, in general, higher, and it drops much slower than for repulsive interactions. It is worth noting that the selectivities calculated for $\omega = 0.4$ and $\omega = 0.6$ decay with increasing time, although the associated kinetic isotherms shown in Figure 1 seem to have already attained plateau values at $t^* = 40$. However, this is only an apparent effect that originates from a short time scale used in Figure 1. In fact, the isotherms obtained for strong attractive interactions change slowly with time even for t^* much larger than 40 (results not shown). As a consequence, as can be seen in Figure 2, the corresponding selectivities decay monotonically even at $t^* = 120$.

On the other hand, we observe that, for $\omega > 1$, S exhibits a minimum that becomes more pronounced when the repulsive interactions grow and when the number of chiral receptor increases (compare the top and the bottom part). Also, in this case, predictions of the MFA are in good agreement with the simulation data, except for the case of strong attractive interactions ($\omega = 0.4$, circles in the bottom part), for which S is overestimated. This is due to the intrinsic properties of the MFA, which works better far from phase transition in the adsorbed phase (larger ω) and also to increasing heterogeneity of the surface (larger f^s), which introduces extra correlations between adsorbed molecules. The observed discrepancy can also be explained by the properties of the isotherms shown in Figure 1. In particular, for $\omega = 0.4$ and $f^s = 0.2$ we observe that the simulated isotherms θ_1 and θ_2 are slightly underestimated and overestimated by the theory, respectively. Consequently, the MFA gives values of S that are too high at small ω.

The results presented so far describe the short-term behavior of our system, and therefore, some of the conclusions are valid only for $t^* \ll \infty$. This is particularly true for the kinetic selectivity obtained for attractive interactions, for which the equilibrium value, S^* is often markedly different from that observed during the initial stage of the adsorption. To illustrate this phenomenon we display in Figure 3 the long-term behavior of S for $\omega = 0.4$ and 1.8. It is clear that the curve corresponding to $\omega = 0.4$ lies above the curve obtained for $\omega = 1.8$ until t^* is less than $\sim$220. At this point the curves crossover. In particular, for the attractive interactions we observe that S decreases continuously with time, while for repulsive interactions it reaches a plateau very quickly. Obviously, in the first case the resulting equilibrium selectivity is lower than S plotted in Figure 1. We will return to this question when discussing equilibrium properties of the separation process.

To further test the validity of the model we also performed simulations corresponding to low concentration of the mixture. This was because many chiral separations by HPLC are performed using relatively dilute solutions, which originates, for example, from a limited solubility of enantiomers. Figure 4 shows the kinetic adsorption isotherms obtained for $c = 0.1$. The results plotted in this figure were obtained for the same values of ω as those used in the calculation of the data presented in Figure 1. In this case, we observe that the influence of lateral interactions on the partial adsorption isotherms is qualitatively similar to the effect already observed for $c = 1$. In particular, for short simulation times the repulsive interactions reduce the efficiency of the separation, that is $|\theta_2 - \theta_1|$ decreases with increasing ω for both values of f^s. Simultaneously, introduction of a larger number of chiral receptors onto the surface increases the difference between θ_1 and θ_2. However, contrary to $c = 1$, for low concentration of the mixture we do not observe a maximum in the adsorption isotherm of the second component. Furthermore, contrary to the data shown in Figure 1, both θ_1 and θ_2 follow the same trend, that is, they decrease with increasing ω.

To examine qualitative changes in the separation that are induced by lowering of the concentration in Figure 5, we plotted kinetic selectivities obtained for $c = 0.1$. For attractive interactions ($\omega = 0.4$ or 0.6) S drops much faster for low than for high concentrations (compare with Figure. 2). Additionally, for $c = 0.1$ the selectivity at $t^* = 120$ is, in general, higher compared to $c = 1$. It is also worth noting that the selectivity calculated for $c = 0.1$

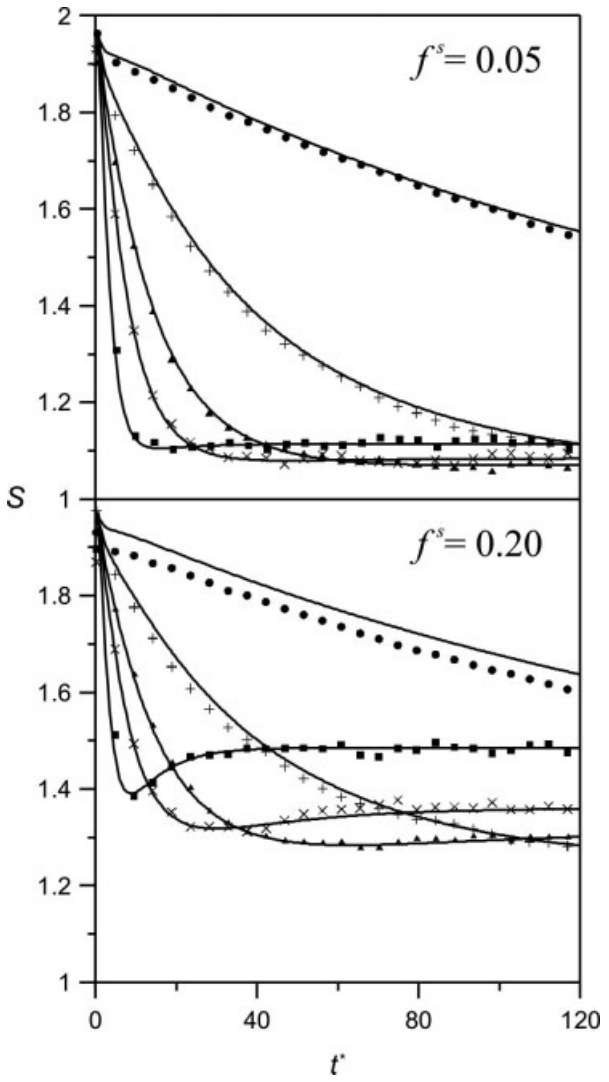

Figure 3. Long-term behavior of the kinetic selectivity, θ_2/θ_1, obtained for $f^s = 0.2$ and for the concentration of the mixture equal to 1. The points are simulation data, whereas the lines are theoretical results calculated using the rate equations. The vertical line in the figure delimits the time interval corresponding to the results shown in this figure.

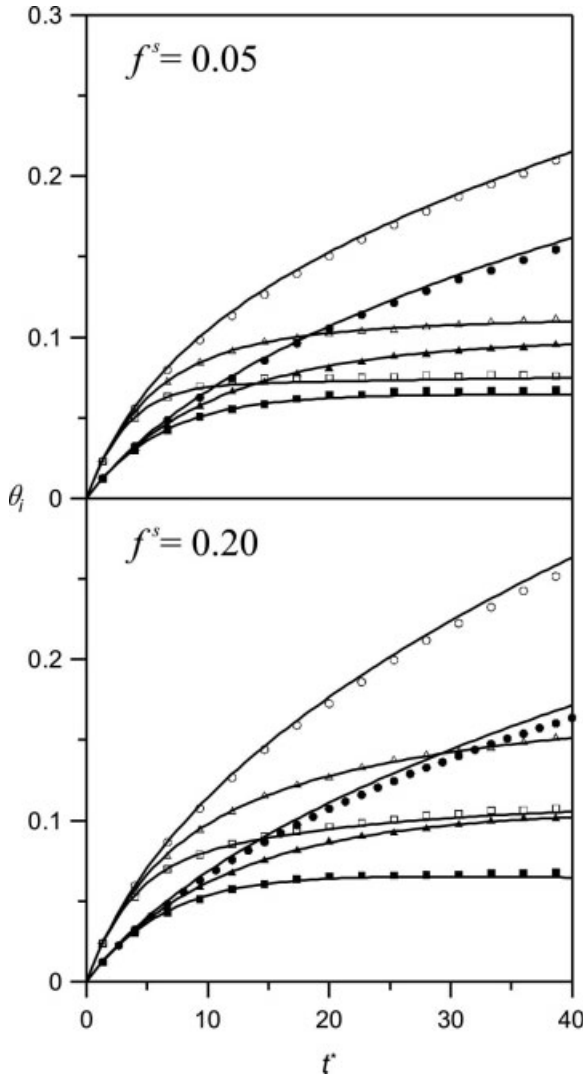

Figure 4. Kinetic adsorption isotherms of components 1 and 2 obtained for different values of the interaction parameter, ω, for the total concentration of the mixture equal to 0.1. The symbols denote simulation data, while the lines are the results obtained by numerical integration of the rate equations. The isotherms shown in both parts were simulated for ω equal to 0.4 (circles), 0.8 (triangles), and 1.8 (squares). The filled and open symbols refer to component 1 and 2, respectively.

increases markedly when f^s changes from 0.05 to 0.2. For example, for $\omega = 1.8$ (squares) we observe that S reaches $\sim$1.2 and $\sim$1.7 for f^s equal to 0.05 and 0.2, respectively. Furthermore, the selectivity obtained for $\omega = 1.8$ and $f^s = 0.2$ exhibits a deep minimum at $t^* \approx 20$. Predictions of the MFA are less accurate for strong attractive interactions, as already observed for $c = 1$.

The next two figures, Figures 6 and 7, we summarize the results discussed above. The first figure shows the equilibrium adsorption isotherms, while the latter presents the associated equilibrium selectivities, which were obtained for $f^s = 0.05$ and $f^s = 0.20$ for different values of ω. In both figures, the symbols denote Monte Carlo data, whereas the lines are numerical solutions of eq. (8). The most striking effect observed in Figure 6 is a noticeable increase of the difference between θ_1^* and θ_2^* associated with an increase of f^s, regardless of the assumed ω (compare the top and the bottom part). Interestingly, the difference increases markedly even for strong attractive interactions ($\omega = 0.4$), for which the effect of f^s on the kinetic isotherms was marginal for short simulation times (see Figure 1). However, as is generally true for the kinetic isotherms, in this case we observe that the presence of repulsive interactions causes both θ_1^* and θ_2^* to drop. Obviously, the opposite effect applies to attractive interactions. It can also be seen from Figure 6 that the stationary solution of the rate equations (lines) agrees well with the Monte Carlo results.

The effect of f^s and ω on the separation of enantiomers is illustrated in a more conclusive way in Figure 7, where it can be

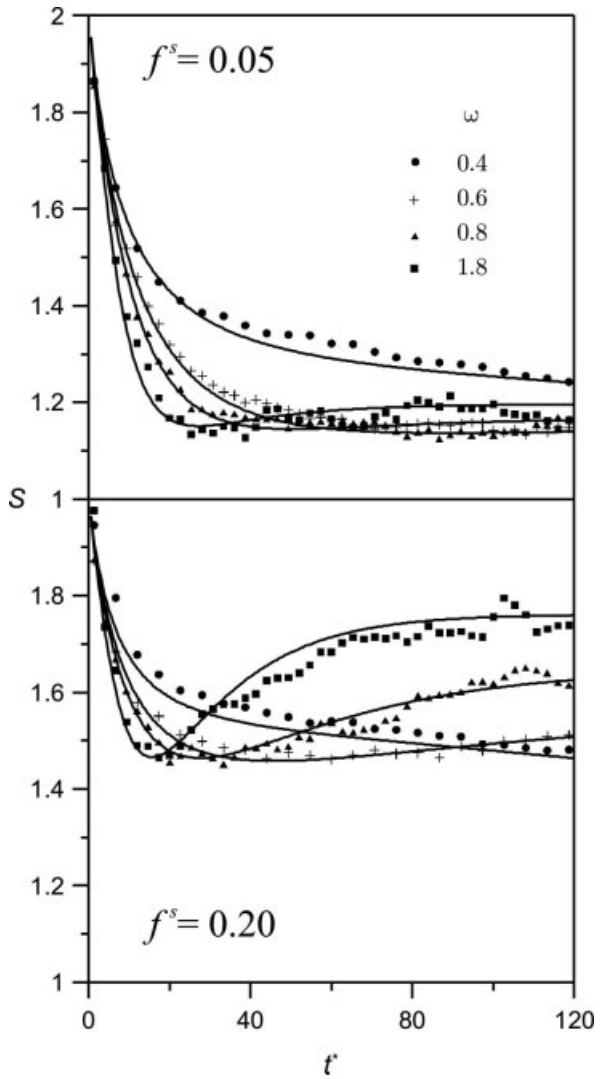

Figure 5. Kinetic selectivity, θ_2/θ_1 as a function of the reduced time, obtained for different values of the interaction parameter ω, for the concentration of the mixture equal to 0.1. The symbols denote simulation data, while the lines are predictions of the theory.

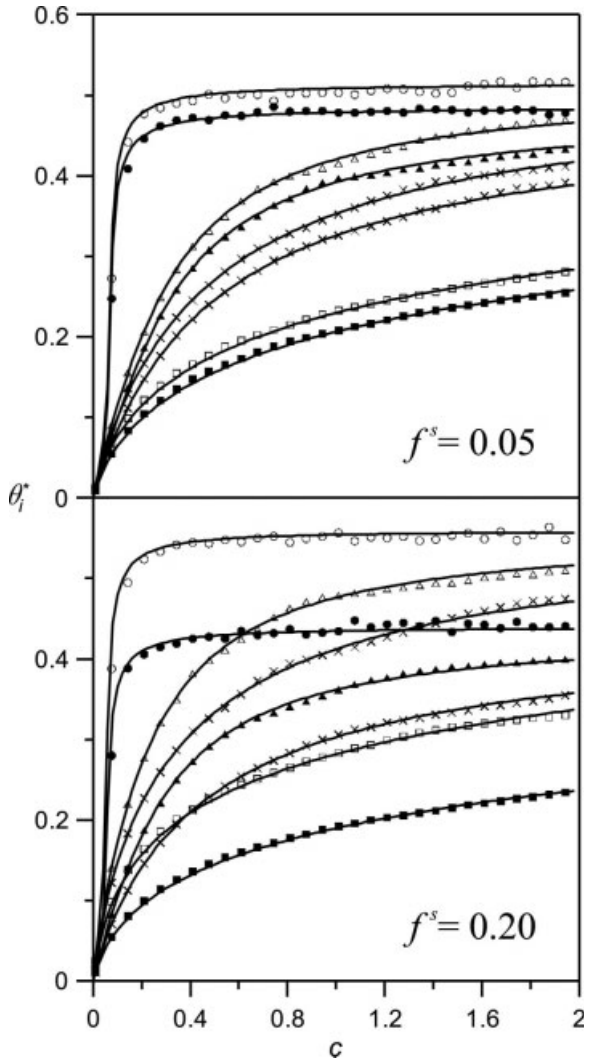

Figure 6. Equilibrium adsorption isotherms of components 1 and 2. The symbols denote simulation data, while the lines were obtained by solving eq. (8). The isotherms shown in both parts were simulated for ω equal to 0.4 (circles), 0.8 (triangles), and 1.8 (squares). The filled and open symbols refer to component 1 and 2, respectively. The additional symbols ($\times$) denote the results obtained assuming lack of interactions between enantiomers ($\omega = 0$).

seen that an increase of the receptor concentration radically improves the equilibrium selectivity. This is particularly easy to notice for low concentrations, at which S^* increases from $\sim$1.3 to $\sim$1.9, regardless of ω (compare the top and the bottom parts). It is worth noting that this initial increase can be explained using intrinsic properties of eq. (8) (limit of low concentrations).[28] Similar, although less intense changes, can also be observed for higher values of c. Moreover, it is evident that attractive interactions reduce the separation at equilibrium—which is in contradiction to the conclusions drawn from the analysis of the initial stages of the adsorption process. For example, in the case of $f^s = 0.20$, we observe that S^* at $c = 1$, drops from $\sim$1.5 to $\sim$1.3 when ω increases from 0.4 to 1.8. As we already mentioned, the kinetic selectivity plotted in Figures 2 and 3 would display a same behavior if t^* were infinitely large.

Conclusions

The results of this work demonstrate that the separation of the components of a racemic mixture by adsorption on CSPs may be strongly influenced by both chiral receptor concentration and the magnitude of lateral interactions between adsorbed enantiomers. We demonstrated that the selectivity in the initial stages may be completely different from the equilibrium value. In particular, the results indicate that, at equilibrium, attractive interactions in the adsorbed phase substantially diminish the selectivity while repulsive interactions enhance it. This conclusion is, however, not valid

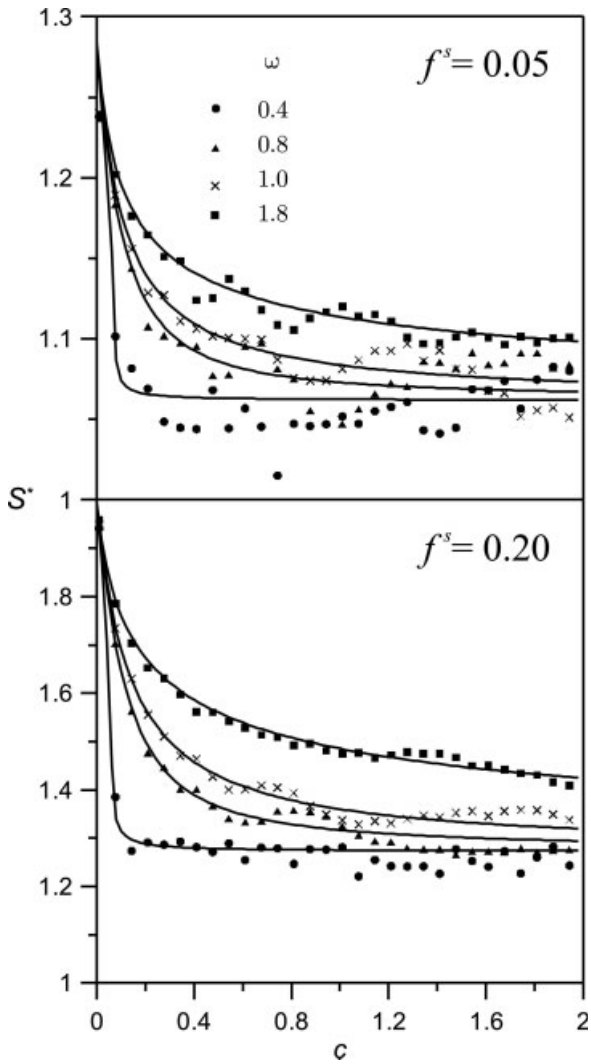

Figure 7. Equilibrium selectivity, θ_2^*/θ_1^* as a function of the concentration of the racemic mixture. The symbols denote simulation data, while the lines were obtained by solving eq. (8).

for the short-term behavior of the system. Consequently, predictions of the selectivity at any instant of time should not be based *a priori* on the equilibrium properties of the system.

The results also indicate that intermolecular interactions may have both a positive as well as a negative influence on the separation process. For example, at equilibrium, repulsive interactions between enantiomers are responsible for enhanced selectivity but, on the other hand, they cause the adsorbed amounts of enantiomers to drop. A practical consequence would be to lower the loading factor of a chromatographic column, reducing the amount of material that can be processed in a time unit. Obviously, an opposite effect would be observed in the case of attractive forces. Optimal conditions for a particular separation by HPLC can, therefore, be obtained by suitably manipulating the receptor concentration and the lateral interactions. This may be achieved by changing the number or spatial distribution of chiral receptors or by changing the nature of interactions between the enantiomers (different solvent, pH, etc.).

Our results demonstrate that the rate equations coupled with the MFA give kinetic and equilibrium adsorption isotherms that are in a good agreement with the results of the MC simulations. This applies particularly to the situation in which attractive forces between adsorbed enantiomers are weak or the temperature is not too low. Taking into account usual conditions at which separation processes are carried out, we believe that the proposed theory can be used for prediction of the kinetic and equilibrium properties of the separation of enantiomers by HPLC.

Acknowledgment

One of the authors (P.S.) is grateful to the Foundation for Polish Science (FNP) for the Award of a Stipend for Young Scientists.

References

1. Horvath, J. D.; Gellman, A. J. J Am Chem Soc 2001, 123, 7953.
2. Ahmadi, A.; Attard, G. Langmuir 1999, 15, 2420.
3. Ferri, D.; Bürgi, T. J Am Chem Soc 2001, 123, 12074.
4. Bonello, J. M.; Lindsay, R.; Santra, A. K.; Lambert, R. M. J Phys Chem B 2002, 106, 2672.
5. Ortega Lorenzo, M.; Haq, S.; Bertrams, T.; Murray, P.; Raval, R.; Baddeley, J. J Phys Chem B 1999, 103, 10661.
6. Zhao, X. J Am Chem Soc 2000, 122, 12584.
7. Ernst, K.-H.; Neuber, M.; Grunze, M.; Ellerbeck, U. J Am Chem Soc 2001, 123, 493.
8. Humblot, V.; Haq, S.; Muryn, C.; Hofer, W. A.; Raval, R. J Am Chem Soc 2002, 124, 503.
9. LeBlond, C.; Wang, J.; Liu, J.; Andrews, A. T.; Sun, Y.-K. J Am Chem Soc 1999, 121, 4920.
10. Guiochon, G.; Shirazi, S. G.; Katti, A. M. Fundamentals of Preparative and Nonlinear Chromatography; Academic Press: Boston, MA, 1994.
11. Ahuja, S. Chiral Separations by Chromatography; Oxford University Press: Washington, DC, 2000.
12. Maier, N. M.; Franco, P.; Lindner, W. J Chromatogr A 2001, 906, 3.
13. Fronstedt, T.; Sajonz, P.; Guiochon, G. J Am Chem Soc 1997, 119, 1254.
14. Cavazzini, A.; Kaczmarski, K.; Szabelski, P.; Zhou, D.; Liu, X.; Guiochon, G. Anal Chem 2001, 73, 5704.
15. Fronstedt, T.; Zhong, G.; Bensetiti, Z.; Guiochon, G. Anal Chem 1996, 68, 2370.
16. Fronstedt, T.; Götmar, G.; Andersson, M.; Guiochon, G. J Am Chem Soc 1999, 121, 1164.
17. Götmar, G.; Fronstedt, T.; Andersson, M.; Guiochon, G. J Chromatogr A 2001, 905, 3.
18. Fu, Q.; Sanbe, H.; Kagawa, C.; Kunimoto, K.-K.; Haginaka, J. Anal Chem 2003, 75, 191.
19. Götmar, G.; Albareda, N. R.; Fronstedt, T. Anal Chem 2002, 74, 2950.
20. Gritti, F.; Guiochon, G. J Colloid Interface Sci 2003, 264, 43.
21. Piatkowski, W.; Gritti, F.; Kaczmarski, K.; Guiochon, G. J Chromatogr A 2003, 989, 207.
22. Vlot, M. S.; Claassen, S.; Huitema, H. E. A.; Van der Erden, J. P. Mol Phys 1997, 91, 19.
23. Largo, J.; Vega, C.; MacDowell, L. G.; Solana, J. R. Mol Phys 2002, 100, 2397.
24. Hill, T. L. An Introduction to Statistical Thermodynamics; Addison–Wesley: Reading, MA, 1960.
25. Talbot, J.; Jin, X.; Wang, N.-H. L. Langmuir 1994, 10, 1663.
26. Ceyrolles, W. J.; Viot, P.; Talbot, J. Langmuir 2002, 18, 1112.
27. Jin, X.; Talbot, J.; Wang, N.-H. L. AIChE J 1994, 40, 1685.
28. Szabelski, P. Appl Surface Sci 2004, 227, 94.